Supplement of Clim. Past, 20, 2617–2628, 2024
https://doi.org/10.5194/cp-20-2617-2024-supplement

Climate of the Past
Open Access
EGU

Supplement of

Precise dating of deglacial Laptev Sea sediments via ^{14}C and authigenic $^{10}Be/^{9}Be$ – assessing local ^{14}C reservoir ages

Arnaud Nicolas et al.

Correspondence to: Arnaud Nicolas (arnaud.nicolas@awi.de) and Florian Adolphi (florian.adolphi@awi.de)

Supplement of

Precise dating of deglacial Laptev Sea sediments via ^{14}C and authigenic $^{10}Be/^{9}Be$ – assessing local ^{14}C reservoir ages

Arnaud Nicolas, Gesine Mollenhauer, Johannes Lachner, Konstanze Stübner, Maylin Malter, Jutta Wollenburg, Hendrik Grotheer, Florian Adolphi

1. Comparison of age-depth models for core PS2458-4

Table S1. Radiocarbon and modelled ages from foraminifera and bivalve samples from core PS2458-4

Depth (cm)	^{14}C Age (^{14}C years)	± (years)	(ΔR= 345 ± 60 ^{14}C years BP)		(ΔR= -110 ± 28 ^{14}C years BP)		Modelled Age (difference) (cal BP)	Sample type	Species
			Modelled Age (mean) (cal BP)	Modelled Age (cal BP, 2σ)	Modelled Age (mean) (cal BP)	Modelled Age (cal BP, 2σ)			
667	12600	110	13745	14089 – 13360	14452	14870 – 14009	707	mb, mbf	*Thyasira* sp., *Yoldiella* sp.
578	12270	65	13198	13428 – 12982	13687	13931 – 13470	489	mb	*Thyasira* sp., *Yoldiella* sp.
530	11560	100	12551	12815 – 12244	12980	13199 – 12748	429	mb	*Thyasira* sp., *Yoldiella* sp.
491*	10968	159	11753	12220 – 11280	12371	12692 – 12026	618	mbf	*L. lobatula, C. neoteretis*
467	10600	75	11291	11630 – 11005	11973	12279 – 11683	682	mb	*Thyasira* sp., *Yoldiella* sp.
399	10090	65	10551	10811 – 10276	11185	11397 – 10991	634	mb	*Thyasira* sp., *Yoldiella* sp.
369	10020	70	10357	10606 – 10135	10966	11187 – 10746	609	mb	*Thyasira* sp., *Yoldiella* sp.
331.5*	9596	122	9860	10183 – 9527	10456	10757 – 10172	596	mbf	*I. helenae, I. norcrossi, C. neoteretis*
291.5*	9089	224	9305	9711 – 8917	9890	10230 – 9529	585	mbf	*C. neoteretis*
252	8830	55	8880	9129 – 8615	9432	9594 – 9258	552	mb	*Thyasira* sp., *Yoldiella* sp.
241.5*	8762	141	8762	9058 – 8448	9310	9527 – 9044	548	mbf	*I. helenae, I. norcrossi, C. neoteretis*
141.5*	6447	158	6334	6696 – 5969	6838	7177 – 6489	504	mbf	*C. neoteretis*
121.5*	6029	134	5985	6297 – 5638	6463	6790 – 6143	478	mbf	*C. neoteretis*
0.5*	0		0					mbf	*C. lobatulus*

Modelled ages were calculated using OxCal4.4 (Ramsey, 2009) with corresponding ΔR values. Marine ^{14}C dates were calibrated with the Marine20 curve (Heaton et al., 2020). The depth values with asterisks represent the new benthic foraminifera samples measured for ^{14}C dates. The depth values without asterisks show the ^{14}C dates published from (Spielhagen et al., 2005).Libby half-life (5568 years) was used to calculate ^{14}C age of foraminifera samples. The modelled age (difference) is calculated by subtracting the modelled age (mean) with ΔR= -110 ± 28 ^{14}C years BP from the modelled age (mean) with ΔR= 345 ± 60 ^{14}C years BP. Sample type: mb= mixed bivalves, mbf= mixed benthic foraminifera.

2. Concentrations of ^{9}Be, ^{10}Be and $^{10}Be/^{9}Be$ atomic ratios from core PS2458-4

Table S2. Mass of ^{9}Be-carrier and concentrations of ^{9}Be, ^{10}Be and $^{10}Be/^{9}Be$ from core PS2458-4

Depth (cm)	Sample Mass (g)	9Be-Carrier (µg)	Authigenic ^{9}Be (at/g) [x10^{16}]	sigma (%)	Be^{10}/Be^{9} (at/at) [x10^{-12}]	sigma (%)	Authigenic ^{10}Be (at/g) [x10^{8}]	sigma (%)	Authigenic $^{10}Be/^{9}Be$ (at/at) [x10^{-8}]	sigma (%)
30	1.00	505	1.10	5.0	2.84	2.0	1.95	2.0	1.77	5.4
70	1.01	504	1.06	5.0	2.63	1.9	1.76	1.9	1.67	5.3
190	1.00	206	2.07	5.5	9.81	2.1	2.06	2.1	0.99	5.9
198	1.00	504	1.14	5.0	1.66	2.4	1.13	2.4	1.00	5.5
200	1.00	204	1.42	5.0	7.19	2.0	1.50	2.0	1.06	5.4
210	1.00	504	1.12	5.0	1.73	1.9	1.17	1.9	1.04	5.4
220	1.00	205	1.34	5.0	6.27	2.0	1.32	2.0	0.99	5.4
230	1.00	208	1.87	5.0	8.30	2.1	1.77	2.1	0.94	5.4
240	1.00	304	1.23	5.0	3.98	2.1	1.24	2.1	1.01	5.4
250	1.00	306	1.43	5.2	4.31	2.0	1.36	2.0	0.95	5.6
260	1.00	306	1.19	7.6	4.10	2.0	1.28	2.0	1.08	7.9
260	1.00	505	0.98	6.0	1.50	2.1	1.02	2.1	1.04	6.3
270	1.00	307	1.26	6.6	3.98	2.0	1.25	2.0	0.99	6.9
280	1.00	306	1.30	5.0	3.85	2.0	1.23	2.0	0.95	5.4
287	1.00	306	1.32	5.0	4.11	2.0	1.27	2.0	0.96	5.4
290	1.00	307	1.41	5.0	4.16	2.0	1.30	2.0	0.93	5.4
300	1.00	505	1.00	5.0	1.36	2.1	0.91	2.1	0.91	5.4
310	1.00	503	1.06	5.0	1.39	1.9	0.93	1.9	0.88	5.4
320	1.00	309	1.19	5.0	3.28	2.2	1.01	2.2	0.85	5.5
320	1.01	500	1.07	5.0	1.42	1.9	0.95	1.9	0.88	5.4
330	1.00	304	1.26	7.0	3.59	2.0	1.10	2.0	0.87	7.3
340	1.00	304	1.38	5.0	3.75	2.1	1.14	2.1	0.83	5.4
350	1.00	304	1.40	5.0	3.60	2.0	1.10	2.0	0.78	5.4
360	1.00	307	1.37	5.0	3.30	2.1	1.01	2.1	0.74	5.4
360	1.00	506	1.02	5.4	1.14	2.0	0.79	2.0	0.78	5.8
370	1.00	302	1.30	5.0	3.23	2.1	0.99	2.1	0.76	5.4
377	1.01	308	1.39	5.0	3.21	2.0	0.98	2.0	0.71	5.4
380	1.00	309	1.38	5.0	3.35	2.0	1.04	2.0	0.76	5.4
390	1.01	308	1.28	5.0	3.02	2.0	0.92	2.0	0.72	5.4
390	1.01	508	1.15	5.0	1.23	1.9	0.83	1.9	0.73	5.4
400	1.00	316	1.29	5.0	2.91	2.1	0.92	2.1	0.71	5.4
405	1.01	313	1.36	10.8	3.29	2.0	1.02	2.0	0.75	11.0
410	1.01	311	0.91	5.0	2.15	2.0	0.66	2.0	0.73	5.4
420	1.00	504	1.12	5.0	1.21	2.0	0.85	2.0	0.76	5.4
430	1.00	509	1.16	5.0	1.24	1.9	0.85	1.9	0.73	5.4
440	1.01	507	1.18	5.0	1.22	2.0	0.82	2.0	0.70	5.4
447	1.01	504	0.98	5.8	1.09	2.0	0.75	2.0	0.76	6.1
450	1.00	507	1.13	5.0	1.10	2.2	0.80	2.2	0.71	5.5
460	1.01	506	1.19	5.0	1.19	2.0	0.80	2.0	0.67	5.4

468	1.01	506	1.41	5.0	1.32	2.0	0.89	2.0	0.63	5.4
487	1.00	508	1.09	5.0	1.08	2.0	0.74	2.0	0.68	5.4
500	1.01	505	1.34	5.0	1.35	2.0	0.91	2.0	0.68	5.4
514	1.00	505	1.12	5.0	1.18	2.0	0.80	2.0	0.72	5.4
514	1.00	505	1.20	5.0	1.25	2.0	0.84	2.0	0.70	5.4
520	1.01	506	1.56	5.0	1.53	2.0	1.03	2.0	0.66	5.4
533	1.00	505	1.17	5.3	1.19	1.9	0.79	1.9	0.67	5.6
550	1.01	506	1.63	5.0	1.57	2.0	1.05	2.0	0.65	5.4
560	1.01	505	1.32	5.0	1.45	2.0	0.97	2.0	0.74	5.4
580	1.01	506	1.50	5.0	1.44	2.0	0.97	2.0	0.64	5.4
600	1.01	505	1.45	5.0	1.33	1.9	0.89	1.9	0.61	5.4
620	1.01	506	1.45	5.0	1.33	2.0	0.89	2.0	0.61	5.4
630	1.00	505	1.24	5.0	1.19	1.9	0.81	1.9	0.65	5.4
640	1.00	506	1.42	5.0	1.24	2.0	0.84	2.0	0.59	5.4
660	1.01	506	1.44	5.0	1.28	2.0	0.86	2.0	0.60	5.4
670	1.01	505	1.54	5.0	1.24	2.0	0.83	2.0	0.54	5.4
680	1.01	505	1.55	5.0	1.29	2.0	0.86	2.0	0.55	5.4
700	1.00	504	1.49	5.0	1.18	2.0	0.80	2.0	0.53	5.4
790	1.00	505	1.15	5.0	1.00	2.0	0.67	2.0	0.59	5.4

3. Replicate samples of $^{10}Be/^{9}Be$ ratios

Table S3. Coefficient of variation values of the replicate samples of $^{10}Be/^{9}Be$ ratios

Depth (cm)	Authigenic $^{10}Be/^{9}Be$ (at/at) [x10^{-8}]	sigma [%]	Authigenic $^{10}Be/^{9}Be$ Coefficient of Variation [%]
260	1.08	7.87	7.11
260	1.04	6.34	
320	0.85	5.46	2.45
320	0.88	5.35	
360	0.74	5.43	3.72
360	0.78	5.75	
390	0.72	5.39	0.98
390	0.73	5.36	
514	0.72	5.37	5.39
514	0.70	5.40	

4. Updated age-depth model for core PS2458-4

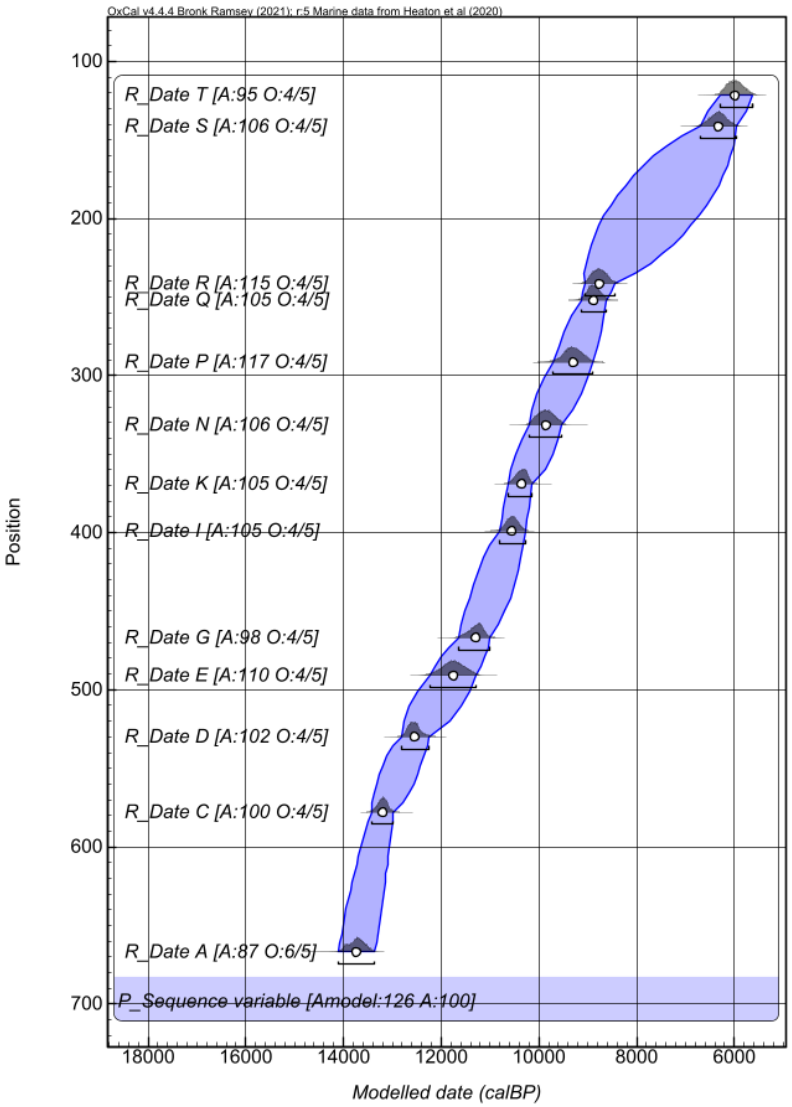

Figure S1. Age-depth model for core PS2458-4 using ΔR value of 345 ± 60 ^{14}C years BP

5. Plot of foraminifera ages with Marine20 and Intcal20

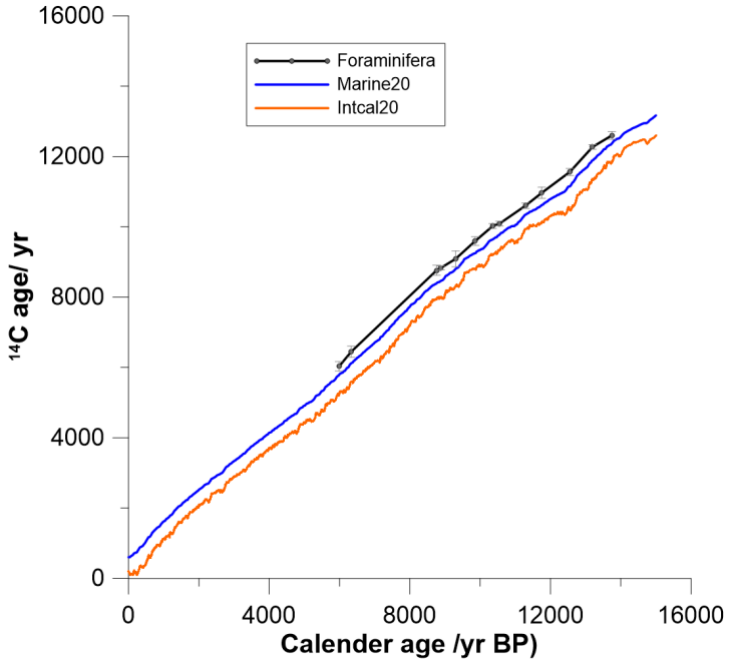

Figure S2. Foraminifera ages plotted with Marine 20 (Heaton et al., 2020) and Intcal20 (Reimer et al., 2020).

6. Marine20 MRA + ΔR vs. Inferred MRA from foraminifera and bivalves samples

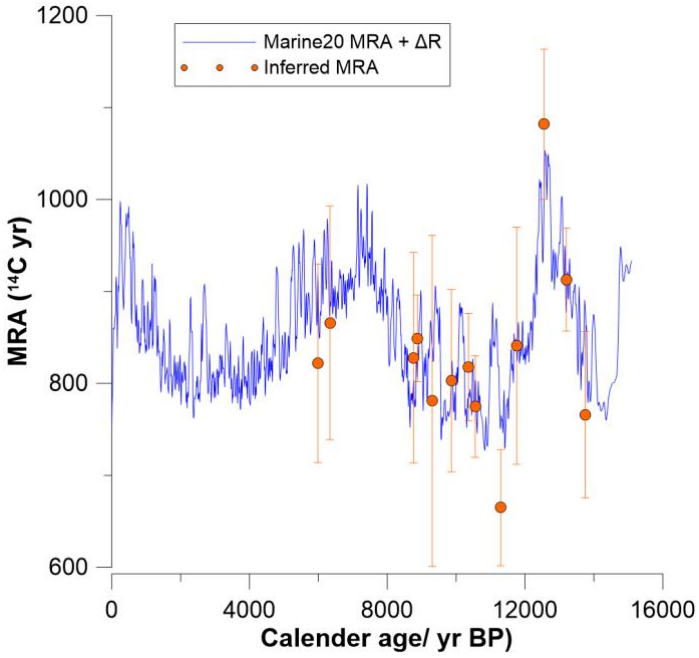

Figure S3. Non-polar global-average MRA corresponding to Marine20 (Heaton et al., 2020) with an added ΔR value of 345 ^{14}C years (blue) and the inferred MRA calculated by subtracting the atmospheric ^{14}C age (derived from Intcal20) from the ^{14}C age of foraminifera.

7. Modelled ice core ^{10}Be time series with a tau value of 200 years

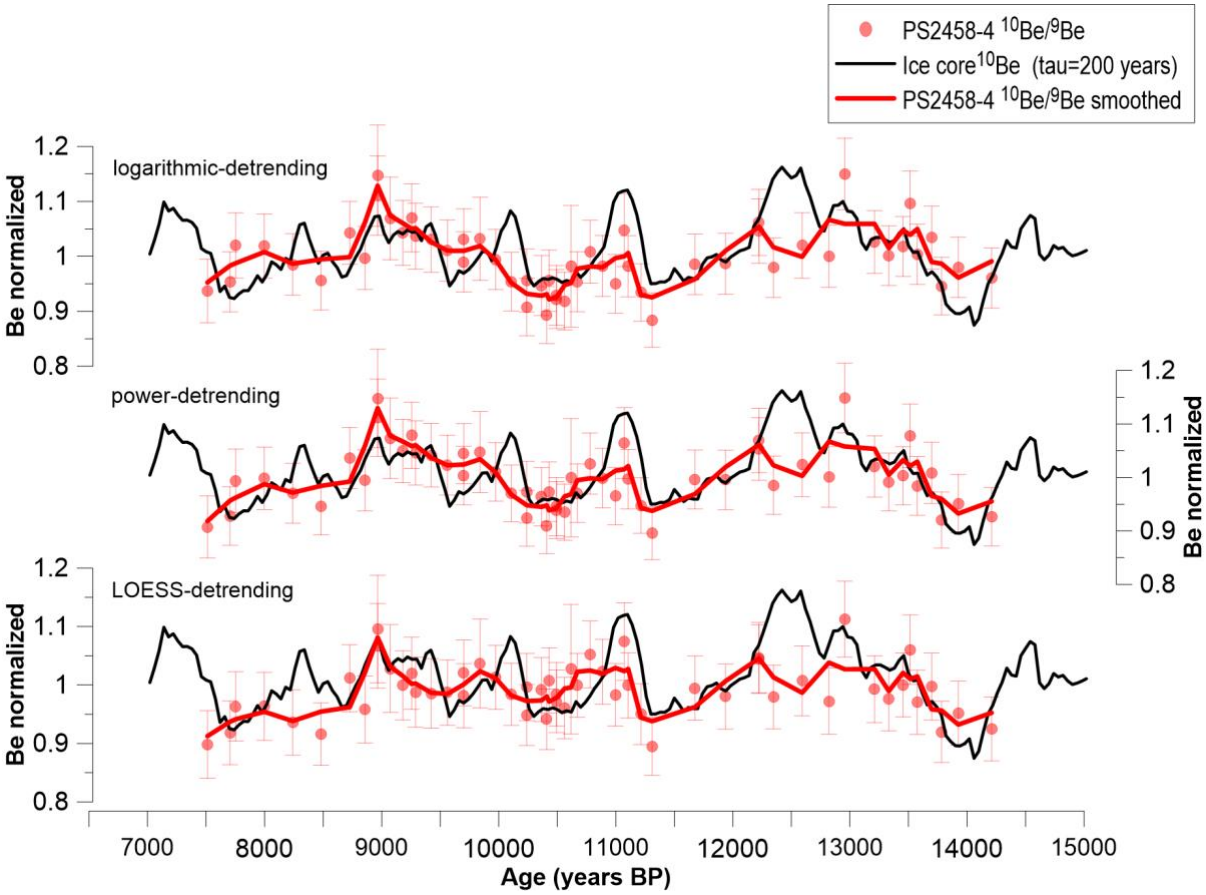

Figure S4. Ice core ^{10}Be record with tau= 200 years (black) with PS2458-4 ^{10}Be/^{9}Be and PS2458-4 ^{10}Be/^{9}Be smoothed data (red) plotted based on logarithmic (upper), power (middle) and LOESS (lower) detrending techniques.

References:

Heaton, T. J., Köhler, P., Butzin, M., Bard, E., Reimer, R. W., Austin, W. E. N., Bronk Ramsey, C., Grootes, P. M., Hughen, K. A., Kromer, B., Reimer, P. J., Adkins, J., Burke, A., Cook, M. S., Olsen, J., and Skinner, L. C.: Marine20 - The Marine Radiocarbon Age Calibration Curve (0-55,000 cal BP), Radiocarbon, 62, https://doi.org/10.1017/RDC.2020.68, 2020.

Ramsey, C. B.: Bayesian analysis of radiocarbon dates, Radiocarbon, 51, https://doi.org/10.1017/s0033822200033865, 2009.

Reimer, P. J., Austin, W. E. N., Bard, E., Bayliss, A., Blackwell, P. G., Bronk Ramsey, C., Butzin, M., Cheng, H., Edwards, R. L., Friedrich, M., Grootes, P. M., Guilderson, T. P., Hajdas, I., Heaton, T. J., Hogg, A. G., Hughen, K. A., Kromer, B., Manning, S. W., Muscheler, R., Palmer, J. G., Pearson, C., Van Der Plicht, J., Reimer, R. W., Richards, D. A., Scott, E. M., Southon, J. R., Turney, C. S. M., Wacker, L., Adolphi, F., Büntgen, U., Capano, M., Fahrni, S. M., Fogtmann-Schulz, A., Friedrich, R., Köhler, P., Kudsk, S., Miyake, F., Olsen, J., Reinig, F., Sakamoto, M., Sookdeo, A., and Talamo, S.: The IntCal20 Northern Hemisphere Radiocarbon Age Calibration Curve (0-55 cal kBP), Radiocarbon, 62, https://doi.org/10.1017/RDC.2020.41, 2020.

Spielhagen, R. F., Erlenkeuser, H., and Siegert, C.: History of freshwater runoff across the Laptev Sea (Arctic) during the last deglaciation, Glob Planet Change, 48, 187–207, https://doi.org/10.1016/j.gloplacha.2004.12.013, 2005.